



Finite element modelling of low energy consumption self-regulating heating floor

H. Desplats & M. Gueguen

*Laboratoire de Génie Mécanique et Matériaux,
Centre de Recherche Sciences de l'Ingénieur, 56325 LORIENT Cedex,
France*

Abstract

Computer models for analyzing heat transfer have been developed for the thermal analysis of a self-regulating heating floor. Self-regulation is due to the conductive polymer composite cables: they are good conductors at low temperatures, and electrical insulators when the temperature increases.

The first calculations, with a two dimensional finite element code, were performed on a piece (one meter square) of heating floating floor made of high density fibre board, under which self-regulating heating cables were placed. The diffusive effect of the aluminium sheet placed between the cables and fibre board is shown. Different widths and thicknesses were tested. Results of the surface temperature are in good agreement with experimentation.

In the second phase, a finite element modelling of the thermo-mechanical behaviour of the self-regulating heating floor, installed in a room, was carried out. Simulations were compared to experimentation. The room wall temperature was regulated: temperature measurements were performed, in particular, between the floor and the ceiling. Heat fluxes exchanged between the floor, the walls and the ceiling were introduced into the model and turbulent convection was modelled by equivalent conductivity. We took into account a turbulent boundary layer of air on the floor. Similar computed and measured temperatures were obtained. An interesting result is the effect of a supplementary energy source (like energy supplied by the sun) on the floor—a decrease in the calculated consumed energy by the cables, due to the local increase in temperature of the cables, is exhibited.

1 Introduction

Low temperature energy systems like heating floors are a contributing factor in reducing energy use. A heating floor is a low temperature heating system. The energy emitted is absorbed by people and objects without directly heating the air, resulting in a comfortable temperature profile between the floor and ceiling. It has long been accepted that for good comfort levels the human body should receive most of its warmth by radiant means, warming the floor means that people experience warm feet and a cool head. The resultant comfort level is achieved at a lower air temperature than that produced by a convection system, and produces no loss of air quality. Water heating and electric heating systems have their own advantages. A water heating system consists of hot water tubes embedded in a concrete slab. Electric heating floor systems, placed under floor panels with lower mass to heat ratio, react faster. Here we consider a special electrical heating floor, a self-regulating one. The advantages of a classical electrical floor heating system are conserved, but self-regulation means that when the ambient temperature rises, the electrical resistance increases and the consumption of electricity decreases. In order to better understand the thermal behaviour of a self-regulating floor and to find the best compromise between cost and performance, finite element modelling has been performed. To start with, we describe the finite element modelling we have developed. Then we present the main characteristics of the self-regulating heating cables and self-regulating heating module. The influence of diffusing aluminium foils in comparison with experimentation is analyzed. An interesting result of self-regulation is shown in the case where an additional energy supply arrives on a self-regulating heating floor. A finite element modelling of heat transfer in a room gives the diminishing consumption in function of additional energy supply.

2 Finite element modelling

A finite element code for the resolution of thermal heat conduction was developed in the laboratory. The equation of heat propagation in stationary conduction can be written as

$$\operatorname{div}(\mathbf{K}_c \cdot \overrightarrow{\operatorname{grad}}T) + r = 0 \quad (1)$$

where T is the temperature, r the volumic source of heat, \mathbf{K}_c the thermal conductivity tensor of the material.

The model was applied to an opaque solid occupying a D domain delimited by a surface ∂D . In weak variational formulation, with the Galerkin method where \dot{T}^* are the virtual temperature time derivatives, the thermal residue R^{th} is given by:

$$R^{th} = - \int_D (\mathbf{K}_c \cdot \overrightarrow{\operatorname{grad}}T)(\overrightarrow{\operatorname{grad}}\dot{T}^*) dV + \int_D r\dot{T}^* dV + \int_{\partial D} (\mathbf{K}_c \cdot \overrightarrow{\operatorname{grad}}T)\dot{T}^* dS. \quad (2)$$

Thermal equilibrium is reached when the residue becomes zero for all virtual temperature time derivatives compatible with the imposed boundary conditions.

Using the finite element approximation scheme, the temperature in the solid can be expressed as a function of mesh nodes with interpolation functions which are the same as those used for the mesh, these are isoparametric interpolations. A mesh attached to the solid is defined by a number $nelt$ finite element, occupying a material domain D in a volume V . Coordinates X^{ar} in direction \vec{I}_a are defined for node number r of element number n . These coordinates can be calculated from a form function $N_r(X^b)$, the interpolation function on a real element, with:

$$\vec{M} = \vec{M}^T N_r(X^b) = X^{ar} N_r(X^b) \vec{I}_a. \quad (3)$$

Functions $N_r(X^b)$ depend on nodes element coordinates. To avoid a large number of calculations of those functions, the reference element notion is used. The parametrization ξ_i attached to this reference element allows the definition of each element point position of the same geometry with unique interpolation functions ϕ_r . The position of one point of the solid is determined from the position of the nodes of the element, to which the point belongs, and from the interpolation function ϕ_r attached to this element.

$$\vec{M} = X^{ar} \phi_r \vec{I}_a. \quad (4)$$

The temperature for any point of the solid is expressed as a function of node temperature, with the same interpolation function as used for the mesh.

$$T = T^r \phi_r. \quad (5)$$

So the matrix form of a null residue is

$$\langle \vec{T}^* | ([K](T) - (Q) + (r)) = 0 \quad (6)$$

where $[K]$ is the symmetrical conductivity matrix, (Q) represents heat fluxes at the surface and (r) is the heat source null every where except in the self-regulating polymer matrix. This system of equations is resolved by the Newton–Raphson method in nonlinear cases. Validations of the code were performed on usual analytical cases and in comparison with the results given by other codes.

3 Self-regulating heating floor element study

3.1 The PTC effect self-regulating cables

Self-regulating cables have been used for several decades for heat tracing include maintaining process fluids at pumpable viscosities, preventing phase change and/or component separation in liquids, and keeping water from freezing when ambient temperatures are sufficiently low. They look like flat cables of nearly 10 mm wide, are laid along the pipe, or sometimes wound round the pipe. Their main characteristic is an electric Joule effect of consumed power which decreases when

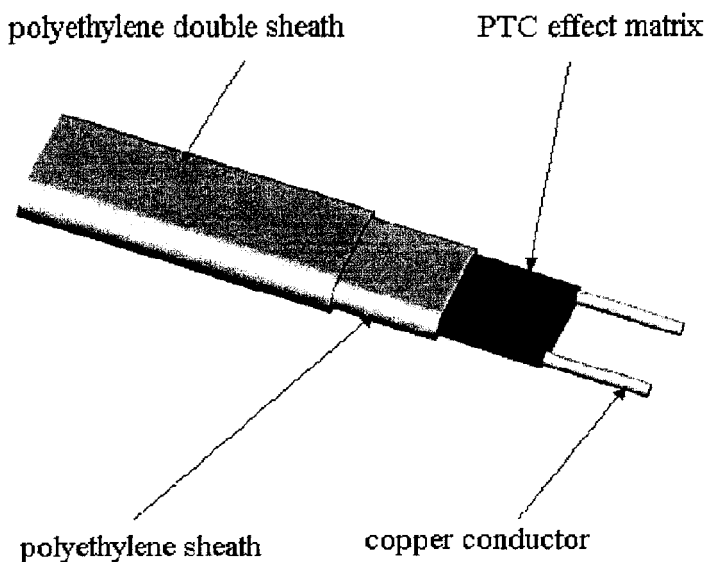


Figure 1: PTC effect heating flat cable.

their temperature increases: so temperature variation of the liquid in the pipe is reduced. At low temperatures, the polymer is a good conductor and the Joule effect heating power is at a maximum when a voltage is applied. When their temperature increases the heating power decreases. This Positive Temperature Coefficient (PTC) effect is observed in heterogeneous polymers with carbon black filler and consists of a rapid increase in the electrical resistance with the temperature increase (until a 10^8 factor for several dozen of degrees Celsius). The transition appears near the polymer's fusion temperature.

3.2 Characteristics of self-regulating cables

See Figure 1. The cable is made of two copper wires (19 strands) of diameter 1.4 mm and spaced 10.3 mm apart. The polyolefin, poly(ethylene-co-alkyl acrylate), with carbon black filler is obtained by extrusion. The variable resistance takes place between the two copper wires. Two high density polyethylene sheaths are also obtained by extrusion, with a thickness of 0.5 mm. This double sheath covering provides physical protection for people and mechanical protection for the cable. Thermal conductivities are taken from the literature, except for the matrix—this value has been measured by CERAP (Centre de Recherche et d'Application des Polymères).

The Joule effect power consumed was measured when 220 V, 50 Hz electricity was applied between the two copper wires. As the temperature varied the power consumed was determined as a function of temperature. Then a straight line was

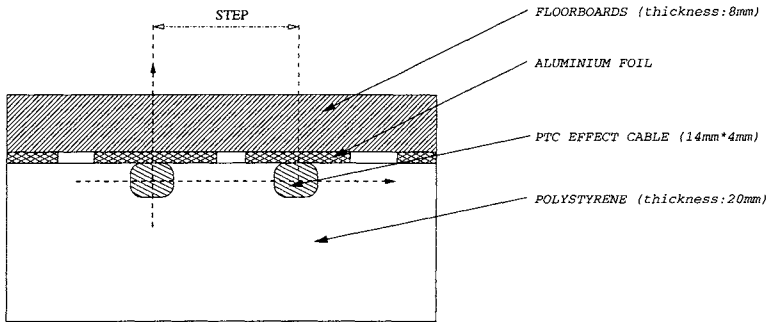


Figure 2: Self-regulating heating cables unit.

obtained, where

$$P(T) = A - BT \quad A > 0, B > 0. \quad (7)$$

From this measured value a volumetric heat power source r is calculated and introduced in the code.

3.3 Experimental study of self-regulating heating module

Tests on the self-regulating heating floor module were carried out in a thermoregulated room: ambient air was controlled at 20 °C (at ± 1.5 °C on wall temperatures). The floor module surface was nearly 1 m². Self-regulating heating cables were set in a polystyrene slab (20 mm thick). Aluminium foil and flooring panels were placed on top. Figure 2 shows a sketch of part of this element, showing the relative material thicknesses. This module was put on a table in the centre of the room. Thermocouples were placed on the surface of the flooring and temperatures were measured in order to estimate surface temperature uniformity and maximum value. French regulations recommend a surface temperature on the floor below 28 °C.

3.4 Main results

3.4.1 Boundary conditions

The volume considered here for finite element modelling was a part of the module delimited by the vertical symmetry plane in the cable and by the vertical plane of symmetry between two cables. Tetrahedrons and hexahedrons are used for meshing. The meshes were made up of nearly 500 elements, depending on studied geometry. On the top surface above the floor and on the bottom surface under the table we have considered both radiative and convective heat fluxes.

Radiative fluxes, between the surfaces of the self-regulating element and the walls and ceiling, can be linearized, because temperatures difference between these surfaces were less than 12 °C. Total emissivity values of the room surfaces and the self-regulating element, considered as grey bodies, were estimated at $\epsilon = 0.9$.

As the dimensions of the room were much larger ($4\text{ m} \times 5\text{ m} \times 2.50\text{ m}$) than those of the element, a radiative exchange coefficient h_r could be defined [1]:

$$h_r = 4\epsilon\sigma T_m^3. \quad (8)$$

Convective exchange factors, for natural convection, were calculated from a Grashoff number Gr with correlation formulae. For different horizontal and vertical surfaces of the element the correlation formulae can be written as

$$Nu = a(PrGr)^b. \quad (9)$$

Values of a and b depend on Grashoff Gr and Prandtl Pr numbers. We have calculated a local Grashoff number then a convective coefficient surface temperature dependant; in the same manner as [2] we found $h_c = 1.50|T - T_{ext}|^{0.33}$ for the upper surface convective coefficient. In our case we have checked that if we took a such temperature variation of convective coefficient, this had no significant effect on temperature results. So we assumed a constant convective coefficient on all the surfaces.

3.4.2 Comparison between tests and simulation

Comparison between tests and simulation were principally made in terms of surface temperature. Conductivities were taken from the literature for usual materials. In order to fit the experimental results, we had to take into account the orthotropy of wood panel conductivity. The presence of an air gap above the cables, due to the laying method, was also modelled.

In the following figures, the effect of the diffusive foils of aluminium is reported. In Figure 3, the effect of the width of the foil is clearly shown. The larger the aluminium foil, better the uniformity was. For a 100 mm large foil, equal to the step between cables, the uniformity was nearly 1°C .

Surface temperature uniformity also increased with the foil thickness. The effect of aluminium foil thickness is shown In Figure 4 for a 70 mm width. For 0.2 mm thick foil, the uniformity was good and if the thickness was increased up to 0.5 mm the uniformity also slowly increased.

The maximum difference temperature is less than 1°C between experimental and numerical results.

4 Self-regulating heating floor in a room

4.1 Experimental set-up

A first test in a quasi-real situation has been performed for heating an upstairs room with self-regulating cables laying under the floor panels. The self-regulating heating floor was installed in a $4\text{ m} \times 2.5\text{ m} \times 2.5\text{ m}$ room. The ground was a 15 cm thick layer of concrete above which the self-regulating floor was placed. It consisted of a 10 cm thick layer of polystyrene on which the cables were placed in the same manner as in the module. The distance between the cables was 90 mm

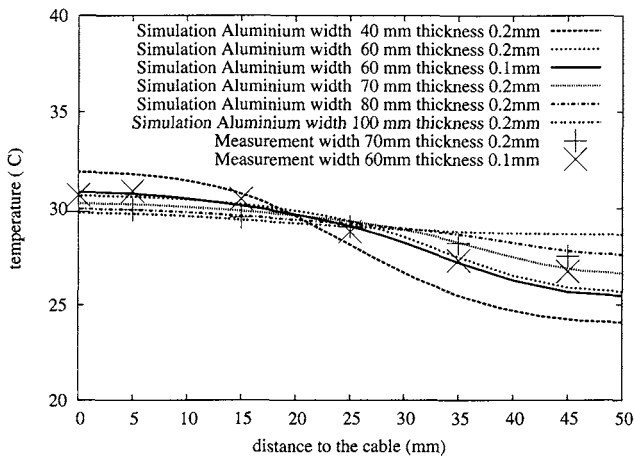


Figure 3: Surface temperature: effect of aluminium foil width.

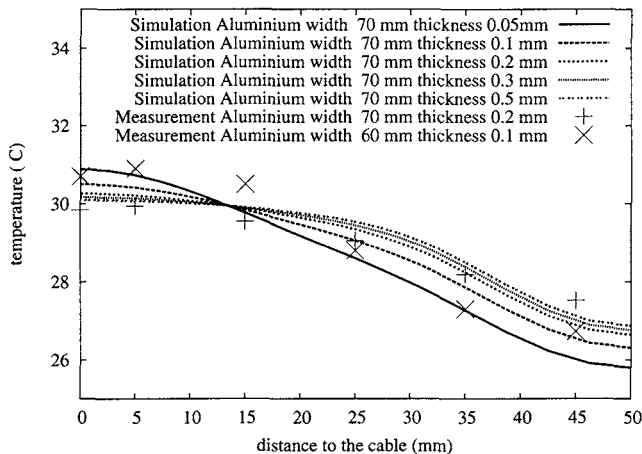


Figure 4: Surface temperature: effect of aluminium foil thickness.

and aluminium foils were placed on the cables. The dimensions of the foils were 0.2 mm thick and 70 mm width. On top the aluminium flooring panels were placed. 40 cables of 2 m length were laid in the width direction of the room.

The walls were made of two wood panels, and cold air flowed between. The walls temperature inside the room was regulated to 14 °C. A ± 1 °C uniformity of temperature was controlled.

The ceiling was plastered, above which a 2.5 cm thick polystyrene slab was placed, and a 20 cm thick glass wool layer was laid above the polystyrene.

4.2 Finite element simulations

The considerations of geometry and thermo-physical properties involve a turbulent natural convection. Hanibuchi and Hokoi [3] describe such a calculation, using a $k - \epsilon$ model for floor heating.

A finite element modelling is being developed as was presented in the previous section. We began to consider a one-dimensional finite element modelling of heat transfer between the floor and its environment. The equation of heat transfer in a solid is resolved in the vertical direction with a linear source of heat in the PTC effect cable. An equivalent source is determined from a previous study. Conduction in the floor and in the ceiling were modelled with conductivities taken to be as in the literature.

The heat transfers in the room are radiative and convective. Radiative exchanges between the floor and ceiling, between the floor and walls (at a constant temperature) and between the ceiling and walls are calculated. Radiative shape factors were calculated, and grey body behaviours were assumed for all surfaces. Outside the room, the external surfaces of the ceiling and of the concrete slab exchanged radiative and convective fluxes with their environment. Heat exchange coefficients were calculated using correlation as below.

An equivalent conductivity λ_{eq} using correlations estimated on the Grashoff number [4] was calculated to take into account turbulent heat transfer between the air room, the floor and the ceiling (distance between floor and ceiling is equal to H). In our conditions for two infinite horizontal planes, the upper plane colder than the lower one, we found $\lambda_{eq} = 170\lambda_{air}$. We assumed the presence of a turbulent thermal boundary layer with thickness $H_{B.L.}$ and conductivity $\lambda_{B.L.}$. Measurements and calculations performed by previous authors indicate a nearly constant vertical temperature over the heating floor, indicating a quasi-null value for the thermal resistance of the turbulent core of air in the room. The boundary layer conductivity $\lambda_{B.L.}$ is calculated from:

$$\frac{H}{\lambda_{eq}} = \frac{H_{B.L.}}{\lambda_{B.L.}} + \frac{H_{turb}}{\lambda_{turb}}. \quad (10)$$

With this relation we assumed a constant thermal resistance of the air room layer between the floor and the ceiling.

4.3 Results of simulations

The thickness of the thermal boundary layer was calculated and measured in [3] and its value was between 5 and 10 cm for a 2.5 m distance between floor and ceiling for a heating floor. It was verified that, if the boundary layer thickness was varied from 5 to 15 cm, the temperature distribution was not significantly changed, see Figure 5.

The effect of supplementary energy absorbed by the floor was evaluated, see Figure 6. For example, an energy supply from sun radiation of 40 W m^{-2} involved a decrease of 10% in electrical consumption of the electrical heating floor. The

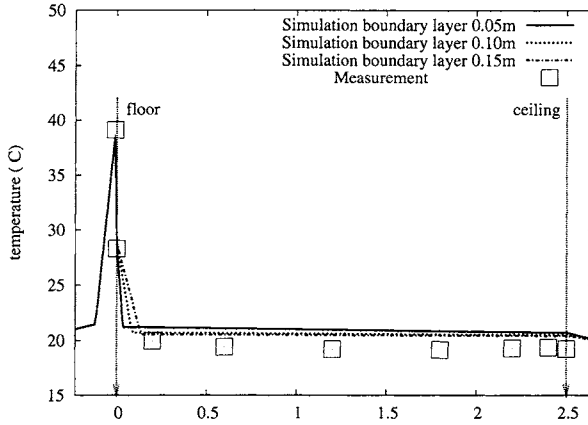


Figure 5: Centre room temperature versus the distance from the floor.

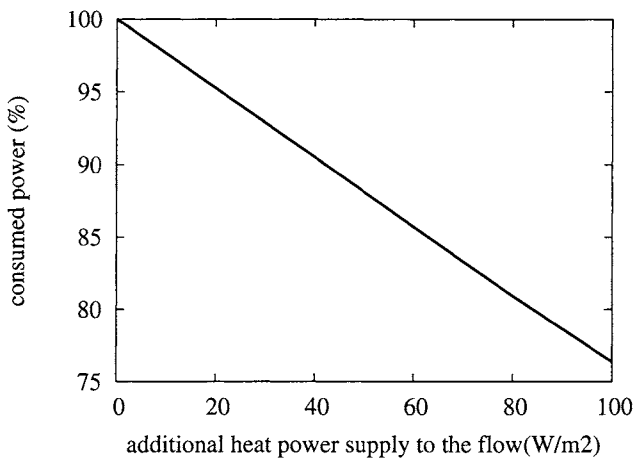


Figure 6: Percentage of consumed electrical power according to additional heat supply.

linear temperature heat transfer in our modelling induced linear decreasing of consumed electrical power.

5 Conclusion and future perspectives

Finite element modelling of a self-regulating heating floor module was realized. The numerical results have been compared to experimentation. The influence of aluminium foil between cables and the floor panels was reported. The surface temperatures of the floor were more uniform as the dimensions of the foil increased.



With a modelling of a complete room with such a heating floor, we showed the diminution of electrical consumption according to an additional flux (like heat from the sun). Some more experimentation has to be performed to confirm the validity of our approach.

Acknowledgement

The authors gratefully acknowledge Jean-Claude Da Rocha, Société Acome at Mortain (Manche), for providing them with the results of the experimental study.

References

- [1] Sacadura, J.F. *Initiation aux transferts thermiques*. Tec & Doc, 1993.
- [2] Caccavelli, D. & Baude, J. Modelling and dimensioning a hot water floor heating system. *Proc. of Building Simulation '95*, pp. 571–579, 1995.
- [3] Hanibuchi, H. & Hokoi, S. A study on radiative and convective heat exchange in a room with floor heating. *Proc. of Building Simulation '99* (Volume 1), pp. 321–328, 1999.
- [4] Taine, J. & Petit J.P. *Transferts thermiques. Cours et données de base. Mécanique des fluides anisothermes*. Editions Dunod, 1994.